HIGH-RESOLUTION STEREO TOPOGRAPHY RE-EXAMINATION OF CENTRAL ARTEMIS, VENUS.

D. C. Nunes[1], S. E. Smrekar[1], Nils Muller[2], Joann Stock[3], Anne Davaille[4], Scott Hensley[1], Kevin Cotton[1], and Karl Mitchell[1]. [1]Jet Propulsion Laboratory, California Institute of Technology (4800 Oak Grove Drive, M/S 183-601, Pasadena CA 91109, Daniel.Nunes@jpl.nasa.gov); [2]German Aerospace Center (DLR), Institute of Planetary Research, Berlin, Germany; [3]California Institute of Technology, Pasadena, CA; [4]Laboratoire FAST, CNRS, Univ. Paris-Sud, Université Paris-Saclay, 91405 Orsay, France.

Introduction: Artemis was first identified by its annular chasma from Pioneer Venus radar altimetry data [1]. Magellan synthetic aperture radar (SAR) images reveals the chasma to contain contractional and extensional tectonic signatures and the interior of Artemis having abundant tectonic and volcanic history. Despite it being classified as a corona based on its volcanotectonic nature and circular aspect [2], its gigantism before all other coronae led to a common belief that, if not a unique corona, Artemis may be a feature in a class of its own. [3, 4] analyzed the tectonic and flexural signatures and interpreted that Artemis suffered contractional folding then extensional rifting of its interior before overthrusting the neighboring lithosphere to the southeast. [5] examined the tectonic features at the central portion of Artemis surrounding Britomartis Chasma and deduced that they are consistent with terrestrial core complexes that occur under spreading regimes. In mapping a broad extent of Venus surrounding Artemis, [6, 7] found that significant tracts contain multiple tectonic elements with orientations geometrically correlated with the shape and position of Artemis, and hypothesized that Artemis is the surface expression of a major mantle upwelling that dominated the geodynamic history of Venus between an early thin-lid regime and a late fracture-zone tectonism.

Here we present a new look at the central portion of Artemis with a newly-derived, soon to be PDS-archived topographic data set that derives from both cross-cycle (Cycle-1/Cycle-3) and intra-cycle (Cycle-1/Cycle-1, Cycle-2/Cycle-2, and Cycle-3/Cycle-3) coverage of the synthetic aperture radar (SAR) images. Specifically, we investigate the topography of the central Britomartis ridge/trough feature and compare it to simple geodynamic models and some terrestrial ocean-floor features.

Stereo Topography: A revitalization of Venus geologic and geodynamic studies for the last ten years derived from new findings from the VIRITIS data set [e.g., 8], continued analysis of previously existing Magellan data products [e.g., 7], and production and analysis of newly derived Magellan products [9]. One of the substantial limitations has been the relatively coarse resolution of the Magellan altimetry data set. [9] stepped up the state of the art by generating a stereo-derived topography dataset based on all Magellan Cycle-1/Cycle-3 coverage, or ~20% of the surface of Venus.

Other prominent stereo digital elevation model (DEM) products to have arisen are those from the USGS [10], but despite their high quality, they cover only a portion of the available cross-cycle coverage. Our approach entails an automatic matching process [11] that has now been tested for several locations of Venus [12, 13], showing an improvement in resolution and absolute elevation benchmarking than [9]. Further, out method also processes intra-cycle stereo data existing from the overlapping strips of successive same-cycle Magellan F-BIDRs [14], which extends DEM coverage to beyond Cycle-I/Cycle-3 coverage. Our DEM presented here is mostly unfiltered, having removed only the most egregious blunders, and without bundle adjustment.

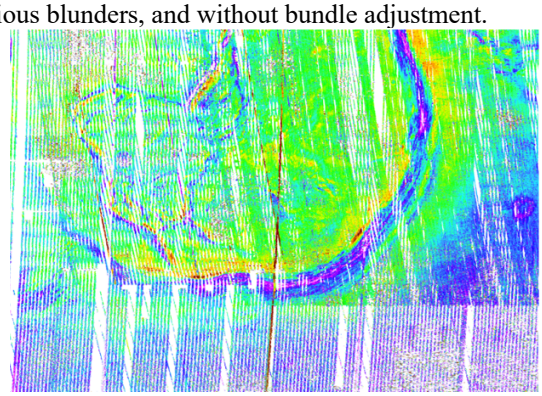

Fig. 1– *Stereo-derived DEM for Artemis from both cross-cycle and intra-cycle SAR (FBIDR) overlaps. DEM covers 120.5°E to 150°E, 30°S to 47°S, with the color scheme stretching from -1000 km to 4000 km in elevation.*

Results: We have built a stereo DEM of Artemis from both cross-cycle and intra-cycle coverage (Fig. 1). Due to on-board hardware issues, Cycle-3 coverage exists only for the eastern half of Artemis and with many gaps. Intra-cycle coverage helps to fill in these gaps and extend the coverage to beyond cross-cycle. The result is a more extensive DEM that achieves higher quality and resolution than in the Magellan Altimetry dataset the stereo DEM of [9]. At central Artemis the intra-cycle contribution is crucial in resolving the ridge and trough of Britomartis. Despite the gaps in stereo that persist even after intra-cycle data is included, our DEM represents an improvement over the previous state of the art (Fig. 2). The ridge/trough set span approximately 25 km across the strike direction from trough to peak, with

elevations ranging -2.5 to 4 km, respectively. This represents a greater relief than that of 5.5 km (-3 to 2.5 km) estimated by [3]. The ridge is asymmetric in cross section, with steeper slopes at its NW face. The overall relief of the tough/ridge remains constant along strike.

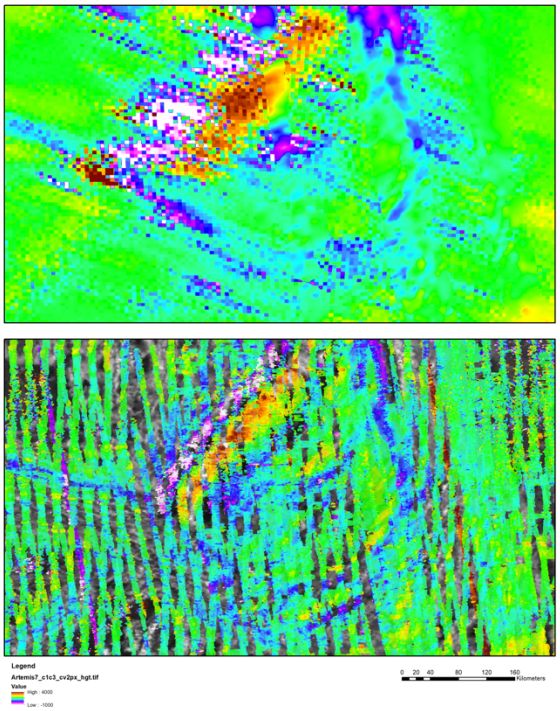

Fig. 2 *– Top: Blended DEM from Cycle-1/Cycle-3 stereo and Magellan altimetry from [9], centered at approximately 132.18°E, 33.35°S. Bottom: Our DEM built from all available cross- and intra-cycle stereo over the same region.*

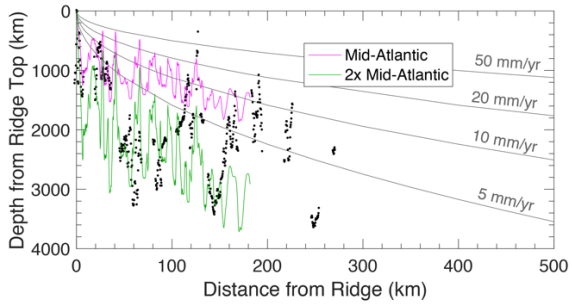

Fig. 3 *– Profile from Britomartis to the SE (dots) compared to halfspace cooling models at different spreading rates and Mid-Atlantic ridge profiles.*

To the southeast of the ridge, the topography decays by nearly 3 km over a baseline of 300 km (Fig. 3). The decay is not monotonic, but instead over a sequence of lesser troughs and ridges, each parallel to the main ridge and a few tens of km across and up to 2.5 km vertically. Such topography does not easily conform to a simple halfspace cooling model and it is not consistent with folding. Instead, it appears to be more similar to what is observed in terrestrial ocean floor away from mid ocean ridges, where ridge-parallel faulting causes substantial variability elevation and is dependent of the magmatic regime [15, 16] . However, the amplitude of the variations found to the SE of Britomartis is twice as much as Mid-Atlantic case we examined (44.92°W, 23.34°N). We selected this specific terrestrial location due to the presence of a well-defined core complex [17]. The hypothesis of a core complex for central Artemis offered by [5] is based on the subtle linear features that extend away and at a high-angle from the Britomartis ridge, as seen in the SAR images and interpreted as grooves. Although subtle in SAR, we believe there is topographic evidence for these grooves as well, especially when looking at the highest stereo resolution data, afforded by the cross-cycle data. Unfortunately, it is at this location where Cycle-3 is noisy and broken, so only a few patches of highest resolution are available. Still, where measurable, the grooves display a relief of a few hundred meters. A VIRTIS anomaly over central Artemis was initially detected [18] based on the GTDR. We are currently assessing this anomaly but have found that the narrowing of the ridge/trough feature due to higher resolution of the stereo DEM makes both the topographic correction and emissivity anomaly less significant.

Discussion: Analysis of our stereo topography is ongoing for Britomartis and the interior deformation in Artemis. At its central portion, the new DEM reveals multiple ridges and troughs associated with the topographic subsidence to the southeast and away from Britomartis. These are subtle to discern in SAR and are similar to faulted blocks in terrestrial spreading centers, albeit larger in amplitude than the specific reference case we used. Groves previously leading to the hypothesis of a core complex are visible in the new DEM. Our findings thus far support an interpretation of a spreading center.

References: [1] Masursky H. et al. (1980) *JGR 85*, 8232-8260. [2] Stofan E.R. et al. (1992) *JGR 97*, 13347-13378. [3] Brown C.D. and R.E. Grimm (1995) *Icarus 117*, 219-249. [4] Brown C.D. and R.E. Grimm (1996) *JGR 101*, 12697-12708. [5] Spencer J.E. (2001) *GSA Bull. 113*, 333-345. [6] Hansen V.L. and I. López (2018) *JGR 123*, 1760-1790. [7] Hansen V.L. and A. Olive (2010) *Geology 38*, 467-470. [8] Smrekar S.E. et al. (2010) *Science 328*, 605-608. [9] Herrick R.R. et al. (2012) *Eos 93*, 125-126. [10] Howington-Kraus E. et al. (2006) *EPSC*, 490. [11] Hensley S. and S. Shaffer (1994) *IGARSS*, 1470-1472. [12] Nunes D.C. et al. (2013) *AGU Fall Meet.*, P41D-1961. [13] Hensley S. et al (2016) *EUSAR*, 1-4. [14] Hensley, S. et al. (2019) *IGARSS,* 6023-6026. [15] Macdonald K.C. et al. (1996) *Nature 380*, 125-129. [16] Sibrant A.L.R. et al. (2018) *Nature Geosci. **11***, 274-279. [17] Whitney D.L. et al. (2013) *GSA Bull. 125*, 273-298. [18] Mueller N. et al. (2008) *JGR 113,* E00B18.